# Supplementary materials

## Temporal and spatial variations in benthic nitrogen cycling in a temperate macro-tidal coastal ecosystem: observation and modeling

Widya Ratmaya*[1], Anniet M. Laverman[2], Christophe Rabouille[3], Zahra Akbarzadeh[4], Françoise Andrieux-Loyer[5], Laurent Barillé[6], Anne-Laure Barillé[7], Yoann Le Merrer[1], Philippe Souchu[1]

[1] Ifremer – LER MPL, Rue de l'Ile d'Yeu, BP 21105, 44311 Nantes Cedex 03, France

[2] Université de Rennes, CNRS, UMR 6553 ECOBIO, Campus Beaulieu, 263 avenue du Général Leclerc, Rennes F-35042, France

[3] Laboratoire des Sciences du Climat et de l'Environnement, CEA-CNRS UNMR 1572, Av. de la Terrasse, 91198 Gif sur Yvette, France

[4] Ecohydrology Research Group, Water Institute and Department of Earth and Environmental Sciences, University of Waterloo, 200 University Avenue West, Waterloo, Ontario, Canada

[5] Ifremer – DYNECO PELAGOS, ZI Pointe du Diable, 29280 Plouzané, France

[6] Université de Nantes, Mer Molécules Santé EA 2160, Faculté des Sciences et des Techniques, BP 92208, 44322 Nantes cedex 3, France

[7] Bio-Littoral, Immeuble Le Nevada, 2 Rue du Château de l'Eraudière CS 80693, 44306 Nantes

* Email: widyaratmaya@gmail.com

Laboratoire Environnement Ressource Morbihan – Pays de la Loire, Centre Ifremer de Nantes, Rue de l'Ile d'Yeu, BP 21105, 44311 Nantes Cedex 03, France.

**Table S1** Reaction network and rate formulation used in the model.

| Description | Reaction formulation[a] | Rate expression[b, c] |
|---|---|---|
| Aerobic respiration | $OM + xO_2 + (2z\text{-}y)HCO_3^- \rightarrow yNH_4^+ + zHPO_4^{2-} + (x\text{-}y+2z)CO_2 + (x\text{-}y+2z)H_2O$ | $R1 = k1\ [OM] \cdot \frac{[O_2]}{[O_2] + kO} \cdot F_T$ |
| Denitrification | $OM + 0.8xNO_3^- \rightarrow 0.4xN_2 + yNH_4^+ + 0.8xNO_2^- + zHPO_4^{2-} + (0.8x+y\text{-}2z)HCO_3^- + (0.2x\text{-}y+2z)CO_2 + (0.6x\text{-}y+2z)H_2O$ | $R2 = k2\ [OM] \cdot \frac{[NO_3^-]}{[NO_3^-] + kNO} \cdot \frac{kinO}{[O_2] + kinO} \cdot 1 - F_{DNRA} \cdot F_T$ |
| DNRA | $OM + 0.5xNO_3^- \rightarrow (0.5x+y)NH_4^+ + (0.5xNO_2^-) + zHPO_4^{2-} + (y\text{-}2z)HCO_3^- + (x\text{-}y+2z)CO_2 + (0.5x\text{-}y+2z)H_2O$ | $R3 = k2\ [OM] \cdot \frac{[NO_3^-]}{[NO_3^-] + kNO} \cdot \frac{kinO}{[O_2] + kinO} \cdot F_{DNRA} \cdot F_T$ |
| Nitrification step 1 | $NH_4^+ + 1.5O_2 \rightarrow NO_2^- + H_2O$ | $R4 = k_{nit1} \cdot \frac{[NH_4^+]}{[NH_4^+] + kmNH4ao} \cdot \frac{[O_2]}{[O_2] + kmO2ao} \cdot F_T$ |
| Nitrification step 2 | $NO_2^- + 0.5O_2 \rightarrow NO_3^-$ | $R5 = k_{nit2} \cdot \frac{[NO_2^-]}{[NO_2^-] + khNIT} \cdot \frac{[O_2]}{[O_2] + khO} \cdot F_T$ |
| Anammox | $NH_4^+ + NO_2^- \rightarrow N_2 + 2H_2O$ | $R6 = k_{anx} \cdot \frac{[NH_4^+]}{[NH_4^+] + khNH4} \cdot \frac{[NO_2^-]}{[NO_2^-] + khNO} \cdot \frac{kinO}{[O_2] + kinO} \cdot F_T$ |

[a] $OM = x(CH_2O)_{org} + y(NH_3)_{org} + z(H_3PO_4)_{org}$, where x, y, z represent the CNP ratios,

[b] $F_{DNRA}$ = fraction of the total nitrate reduction occurring via DNRA (5%),

[c] $F_T$ = temperature correction for the rates. $F_T = \frac{K_1 \cdot exp(\gamma_1 \cdot (T - T_1))}{1 + K_1 \cdot exp(\gamma_1 \cdot (T - T_1) - K_1} \cdot \frac{K_2 \cdot exp(\gamma_2 \cdot (T_2 - T)}{1 + K_2 \cdot exp(\gamma_2 \cdot (T_2 - T) - K_2}$, where $T_1$ and $T_2$ are the lower and upper temperature for the OM decay, respectively; $K_1$ and $K_2$ are the coefficient rates for the lower and upper temperature, respectively; $\gamma_1$ and $\gamma_2$ are the temperature rate multipliers for $T_1$ and $T_2$, respectively (see Cole and Wells, 2006 for details).

**Table S2** Boundary conditions used in the model.

| Parameters | Apr 15th | Apr 22nd | Jun 16th | Jun 24th | Aug 5th | Sep 8th | St. A | St. B | St. C | St. D | Unit | Sources |
|---|---|---|---|---|---|---|---|---|---|---|---|---|
| | 2015 (Nord Dumet monitoring station/St. A) | | | | | | 2016 | | | | | |
| *Solutes* | | | | | | | | | | | | |
| $O_2$ | 142 (84%) | 161 (95%) | 142 (82%) | 120 (75%) | 118 (93%) | 114 (101%) | 198 (80%) | 96 (37%) | 170 (70%) | 198 (79%) | µM | I |
| $NO_3^-$ | 17.7 | 13.1 | 1.60 | 1.30 | 0.07 | 0.04 | 0.37 | 6.82 | 0.20 | 0.47 | µM | I |
| $NO_2^-$ | 0.27 | 0.26 | 0.12 | 0.17 | 0.03 | 0.03 | 0.04 | 0.73 | 0.00 | 0.06 | µM | I |
| $NH_4^+$ | 1.90 | 3.30 | 1.03 | 1.23 | 0.21 | 0.09 | 0.80 | 4.40 | 1.80 | 1.61 | µM | I |
| $Fe^{2+}$ | 0 | 0 | 0 | 0 | 0 | 0 | 0 | 0 | 0 | 0 | µM | I |
| $SO_4^{2-}$ [a] | 28 | 28 | 28 | 28 | 28 | 28 | 28 | 28 | 28 | 28 | mM | M |
| *Solids* | | | | | | | | | | | | |
| OM1 | 600 | 600 | 700 | 750 | 275 | 375 | 1,500 | 1,800 | 1,000 | 400 | µmol C $cm^{-2}$ $yr^{-1}$ | M |
| OM2 | 150 | 150 | 170 | 180 | 120 | 120 | 300 | 300 | 300 | 150 | µmol C $cm^{-2}$ $yr^{-1}$ | M |
| $Fe(OH)_3$ | 75 | 75 | 75 | 75 | 75 | 75 | 75 | 75 | 75 | 75 | µmol $cm^{-2}$ $yr^{-1}$ | M |

Solute concentrations were obtained from the measurements. Solid fluxes were constrained from the model fitting (see Methods). [a] The $SO_4^{2-}$ concentration was constrained from the measured salinity. Sources: **M**, constrained by the model fitting; **I**, independently determined from the field data.

**Table S3** Reaction parameter values used in the model.

| Parameters | Apr 15th | Apr 22nd | Jun 16th | Jun 24th | Aug 5th | Sep 8th | St. A | St. B | St. C | St. D | Unit | Source | Ref. | Description |
|---|---|---|---|---|---|---|---|---|---|---|---|---|---|---|
| | 2015 (Nord Dumet monitoring station/St. A) | | | | | | 2016 | | | | | | | |
| *Fixed* | | | | | | | | | | | | | | |
| C:N OM1 | 10 | 10 | 10 | 10 | 10 | 10 | 10 | 10 | 10 | 10 | | M | | C:N ratio for OM1 |
| C:N OM2 | 15 | 15 | 15 | 15 | 15 | 15 | 15 | 15 | 15 | 15 | | M | | C:N ratio for OM2 |
| $k_O$ | 5 | 5 | 5 | 5 | 5 | 5 | 5 | 5 | 5 | 5 | µM | L | 2, 4, 5 | Limitation of $O_2$ for aerobic oxidation |
| $k_{NO}$ | 5 | 5 | 5 | 5 | 5 | 5 | 5 | 5 | 5 | 5 | µM | L | 2, 4, 5 | Limitation of $NO_3^-$ for denitrification |
| $k_{mNH4ao}$ | 5 | 5 | 5 | 5 | 5 | 5 | 5 | 5 | 5 | 5 | µM | L | 1 | Limitation of $NH_4^+$ for nitrification step 1 |
| $k_{mO2ao}$ | 5 | 5 | 5 | 5 | 5 | 5 | 5 | 5 | 5 | 5 | µM | L | 1 | Limitation of $O_2$ for nitrification step 1 |
| $k_{hNIT}$ | 1 | 1 | 1 | 1 | 1 | 1 | 1 | 1 | 1 | 1 | µM | L | 1 | Limitation of $NO_2^-$ for nitrification step 2 |
| $k_{HO}$ | 5 | 5 | 5 | 5 | 5 | 5 | 5 | 5 | 5 | 5 | µM | L | 1 | Limitation of $O_2$ for nitrification step 2 |
| $k_{hno}$ | 1 | 1 | 1 | 1 | 1 | 1 | 1 | 1 | 1 | 1 | µM | L | 3 | Limitation of $NO_2^-$ for anammox |
| $k_{hnh}$ | 1 | 1 | 1 | 1 | 1 | 1 | 1 | 1 | 1 | 1 | µM | L | 3 | Limitation of $NH_4^+$ for anammox |
| $k_{inO}$ | 6 | 6 | 6 | 6 | 6 | 6 | 6 | 6 | 6 | 6 | µM | L | 6 | Inhibition of $O_2$ for anoxic processes |
| $k_1$ OM1 | 16 | 16 | 16 | 16 | 16 | 16 | 16 | 16 | 16 | 16 | $yr^{-1}$ | M | | Rate constant for aerobic oxidation of OM1 |
| $k_1$ OM2 | 0.1 | 0.1 | 0.1 | 0.1 | 0.1 | 0.1 | 0.1 | 0.1 | 0.1 | 0.1 | $yr^{-1}$ | M | | Rate constant for aerobic oxidation of OM2 |
| $k_2$ OM1 | 5 | 5 | 5 | 5 | 5 | 5 | 5 | 5 | 5 | 5 | $yr^{-1}$ | M | | Rate constant for denitrification and DNRA of OM1 |
| $k_2$ OM2 | 0.1 | 0.1 | 0.1 | 0.1 | 0.1 | 0.1 | 0.1 | 0.1 | 0.1 | 0.1 | $yr^{-1}$ | M | | Rate constant for denitrification and DNRA of OM2 |
| *Adjusted* | | | | | | | | | | | | | | |
| $k_{nit}$ 1 | 90 | 80 | 180 | 180 | 100 | 190 | 20 | 5 | 50 | 60 | µmol $cm^{-3}$ $yr^{-1}$ | M | | Maximum rate for nitrification step 1 |
| $k_{nit}$ 2 | 200 | 195 | 550 | 550 | 400 | 540 | 30 | 50 | 190 | 150 | µmol $cm^{-3}$ $yr^{-1}$ | M | | Maximum rate for nitrification step 2 |
| $k_{anx}$ | 0.03 | 0.05 | 0.02 | 0.02 | 0.04 | 0.02 | 0.02 | 0.02 | 0.02 | 0.02 | µmol $cm^{-3}$ $yr^{-1}$ | M | | Maximum rate for anammox |
| *Measured* | | | | | | | | | | | | | | |
| Ø | 0.83 | 0.84 | 0.88 | 0.85 | 0.85 | 0.82 | 0.87 | 0.92 | 0.59 | 0.40 | $cm^3$ $cm^{-3}$ | I | | Sediment porosity |
| ρ | 2.89 | 2.49 | 3.26 | 2.74 | 3.08 | 3.06 | 2.71 | 4.45 | 2.50 | 1.93 | g $cm^{-3}$ | I | | Sediment density |
| T° | 11.1 | 11.9 | 14.4 | 14.9 | 17.9 | 17.8 | 16.5 | 13.8 | 17.3 | 15.8 | °C | I | | Bottom water temperature |

The sources of the parameter values are indicated by the following codes: **M**, constrained by the model fitting; **I**, independently determined from the field data, **L**, literature value, with references given as follows: 1. Ward (1986); 2. Wang and VanCappellen (1996); 3. Dalsgaard and Thamdrup (2002); 4. Canavan et al. (2006); 5. Dale et al. (2016); 6. Akbarzadeh et al. (2018).

**Table S4** Model parameter values for the transport processes that were invariable within the season and sampling station.

| Parameters | Value | Description | Unit | Sources |
|---|---|---|---|---|
| Db | 3 | Bioturbation coefficient at $x < 2$ cm | $cm^2\ yr^{-1}$ | M |
| | 1.5 | Bioturbation coefficient at $2\ cm \leq x \leq 4$ cm | $cm^2\ yr^{-1}$ | M |
| | 0.3 | Bioturbation coefficient at $4\ cm \leq x \leq 7$ cm | $cm^2\ yr^{-1}$ | M |
| | 0.1*(1 - exp(x - 20)) | Bioturbation coefficient at $x > 7$ cm | $cm^2\ yr^{-1}$ | M |
| α | 3 | Bioirrigation coefficient at $x < 2$ cm | $yr^{-1}$ | M |
| | 1.5 | Bioirrigation coefficient at $2\ cm \leq x \leq 4$ cm | $yr^{-1}$ | M |
| | 0.3 | Bioirrigation coefficient at $4\ cm \leq x \leq 7$ cm | $yr^{-1}$ | M |
| | 0.1*(1 - exp(x - 20)) | Bioirrigation coefficient at $x > 7$ cm | $yr^{-1}$ | M |
| ω | 0.5 | Burial velocity | $cm\ yr^{-1}$ | M |

See Table S2 for the source indications

## Characteristic time-scales for the sediment processes

*1. Diffusion time-scale*

Diffusion time-scales calculated from the modified Einstein-Smoluchowski equation (Jørgensen and Revsbech, 1985):

$$t_{DIFF} = z^2/2D_s \quad \text{eq. 1}$$

where $t_{DIFF}$ is the diffusion time-scales (d), $z$ is the characteristic length (cm), and $D_s$ is the diffusion coefficient ($cm^2\ s^{-1}$), corrected with the bottom water temperature and sediment porosity for each measurement. The diffusion time-scale was calculated for the upper 2 cm layer, where the exchange between the sediment and overlying water occurs most actively.

**Table S5** Diffusion time-scales for $NH_4^+$, $NO_3^-$ and DON over the first 2 cm sediment layer.

| Date | $D_s$ $NH_4^+$ | $D_s$ $NO_3^-$ | $D_s$ DON* | $t_{DIFF}$ $NH_4^+$ | $t_{DIFF}$ $NO_3^-$ | $t_{DIFF}$ DON |
|---|---|---|---|---|---|---|
| | | (x $10^{-6}$ $cm^{-2}$ $s^{-1}$) | | | (*d*) | |
| April 15th. | 1.4 | 1.4 | 0.17 | 1.6 | 1.7 | 13.2 |
| April 22nd | 1.4 | 1.4 | 0.18 | 1.6 | 1.6 | 13.2 |
| June 16th | 1.5 | 1.5 | 0.19 | 1.5 | 1.5 | 12.4 |
| June 24th | 1.6 | 1.5 | 0.19 | 1.5 | 1.5 | 12.5 |
| August 5th | 1.7 | 1.6 | 0.21 | 1.4 | 1.4 | 11.3 |
| September 8th | 1.7 | 1.6 | 0.21 | 1.4 | 1.4 | 11.1 |

$t_{DIFF}$ = the diffusion time-scale; Ds = the diffusion coefficient. *The $D_s$ of DON was estimated using the empirical relationship between the free solution diffusion coefficient (Do) and the molecular weight (MW) for the various organic compounds at 25°C in distilled water reported by Burdige et al. (1992), assuming a fixed average MW of 2500 Daltons. The obtained values were then corrected for in situ temperature using the Stoke-Einstein equation and translated to Ds after correction for sediment porosity (Boudreau, 1997).

*2. Residence time of the solutes*

The residence time of the solutes at steady-state can be calculated by dividing the stock of the solutes by the flux of these solutes.

$$t_{RES} = Stock/DifFlux \quad \text{eq. 2}$$

where $t_r$ is the residence time of the solutes (d), *Stock* is the average stock of the solutes over the first 2 cm sediment layer (µmol $m^{-2}$), and *DifFlux* is the diffusive fluxes of the solutes (µmol $m^{-2}$ $d^{-1}$).

**Table S6** Residence time of $NH_4^+$, $NO_3^-$ and DON over the first 2 cm sediment layer.

| Date | Stock | | | DifFlux | | | $t_{RES}$ | | |
|---|---|---|---|---|---|---|---|---|---|
| | $NH_4^+$ | $NO_3^-$ | DON | $NH_4^+$ | $NO_3^-$ | DON | $NH_4^+$ | $NO_3^-$ | DON |
| | (µmol $m^{-2}$) | | | (µmol $m^{-2}$ $d^{-1}$) | | | (*d*) | | |
| April 15th. | 3,138 | 376 | 7,473 | 427 | -247 | 148 | 7.4 | 1.5 | 50 |
| April 22nd | 3,699 | 294 | 8,156 | 541 | -99 | 157 | 6.8 | 3.0 | 52 |
| June 16th | 3,487 | 130 | 6,471 | 518 | 17 | 175 | 6.7 | 7.5 | 37 |
| June 24th | 2,858 | 198 | 9,469 | 439 | 44 | 225 | 6.5 | 4.5 | 42 |
| August 5th | 3,384 | 84 | 6,322 | 589 | 21 | 193 | 5.7 | 4.1 | 33 |
| September 8th | 3,795 | 113 | 6,916 | 567 | 22 | 212 | 6.7 | 5.2 | 33 |

* Diffusive fluxes calculated from the concentration gradient at the SWI using Fick's first law of diffusion (Boudreau, 1997; Schulz, 2006)

## Sensitivity analysis

The sensitivity analysis was carried out by imposing changes in the model boundary condition (Table S3) and parameter values (Table S2 & S4) for each sampling date. The contribution of $NO_2^-$ to the DIN fluxes was considered negligible (< 5% of the $NH_4^+$ and $NO_3^-$ fluxes) and therefore not included in the sensitivity analysis. A stepwise approach was applied by manually changing the parameter values individually (Table S7) and observing the model response on the $NH_4^+$ and $NO_3^-$ fluxes. The model was run by imposing each change in these values one by one for each sampling date. A combination effect between the parameters was not tested in the sensitivity analysis in the present study. The response was calculated as a percentage of change in the $NH_4^+$ and $NO_3^-$ fluxes with regard to best fits (baseline model).

**Table S7** List of tested parameters for the sensitivity analysis.

| Parameters | Description |
|---|---|
| Anoxic | Bottom water $O_2$ concentrations are equal to zero |
| BW $NO_3^-$ = 10x (100x) | Increase in the bottom water $NO_3^-$ concentrations by 10 fold (or 100 fold for August and September) |
| OM1 2x (3x) | Increase in the deposition of OM1 by 2 fold (or 3x for August) |
| OM1 <=> OM2 | Inversing the proportion of OM1 and OM2 |
| $k_1$ OM1 = 2x | Increase in the rate constant for the aerobic oxidation of OM1 by 2 fold |
| $k_1$ OM1 = 1/2 x | Decrease in the rate constant for the aerobic oxidation of OM1 by one-half |
| C/N OM1 = 106/16 | Imposed change in the C/N ratio compared to that in living phytoplankton (i.e., Redfield ratio) |
| Db = 10x | Increase in the bioturbation coefficient by 10 fold |
| $\alpha$ = 10x | Increase in the bioirrigation coefficient by 10 fold |

**Table S8** Density of macrofauna in the incubated sediment cores of the temporal study carried out at the ND monitoring station in 2015.

| Species names | Apr 15th | Apr 22nd | Jun 16th | Jun 24th | Aug 5th | Sep 8th | Total species/m$^2$ |
|---|---|---|---|---|---|---|---|
| Crustacea | | | | | | | |
| *Asthenognathus atlanticus* | 1 | 2 | | | | | 78 |
| *Philocheras bispinosus bispinosus* | | | 1 | | | | 26 |
| Echinoderms | | | | | | | |
| *Acrocnida brachiata* | 1 | | | | 1 | | 52 |
| ***Amphiura filiformis*** | 6 | 6 | 4 | 22 | | 6 | 1,146 |
| *Labidoplax digitata* | | | | | 2 | | 52 |
| *Leptopentacta elongata* | | | 1 | 2 | 2 | | 130 |
| *Synaptidae* | | | | | | | |
| Molluscs | | | | | | | |
| *Abra nitida* | | | 1 | | 2 | 1 | 104 |
| *Corbula gibba* | | 1 | | | | | 26 |
| *Kurtiella bidentata* | 5 | | 1 | 3 | | 4 | 339 |
| *Nassarius pygmaeus* | | | | | 1 | 1 | 52 |
| ***Nucula nitidosa*** | 27 | 27 | 15 | 24 | 3 | 5 | 2,631 |
| *Philine aperta* | | | | 1 | 2 | | 78 |
| *Spisula solida* | 1 | | | | | | 26 |
| *Turritella communis* | | | | 1 | 1 | | 52 |
| Annelids | | | | | | | |
| *Aphelochaeta* | | | | | | 1 | 26 |
| *Chaetozone* | | | | | | 1 | 26 |
| *Glycera unicornis* | 1 | | | | | 1 | 52 |
| *Heteromastus filiformis* | | 2 | | | | 6 | 208 |
| *Labioleanira yhleni* | 1 | 4 | 2 | 2 | 1 | | 260 |
| *Magelona* | | | 1 | | 4 | | 130 |
| Maldanidae | | 1 | 1 | 4 | 1 | | 182 |
| *Malmgrenia lilianae* | 3 | 1 | | 3 | | | 182 |
| *Nephtys* | 1 | 1 | | | | | 52 |
| *Pholoe baltica* | | | 1 | 1 | | | 52 |
| ***Sternaspis scutata*** | 5 | 3 | 5 | 1 | 8 | | 573 |
| Cnidaria | | | | | | | |
| *Edwardsidae* | | | | | 1 | | 26 |
| *Halcampa* | | | | | | | |
| *Virgularia* | | | | | 1 | 4 | 130 |
| Others | | | | | | | |
| *Nemertea* | | 2 | 1 | | | 1 | 104 |
| *Phoronidien* | | 1 | | | | 1 | 52 |

* Sediment core surface area = 64 cm$^2$

## References


Akbarzadeh, Z., Laverman, A.M., Rezanezhad, F., Raimonet, M., Viollier, E., Shafei, B., Van Cappellen, P., 2018. Benthic nitrite exchanges in the Seine River (France): An early diagenetic modeling analysis. Sci. Total Environ. 628-629, 580-593. https://dx.doi.org/10.1016/j.scitotenv.2018.01.319.

Boudreau, B.P., 1997. Diagenetic Models and Their Implementation : Modelling Transport and Reactions in Aquatic Sediments. Springer-Verlag, Berlin.

Burdige, D.J., Alperin, M.J., Homstead, J., Martens, C.S., 1992. The role of benthic fluxes of dissolved organic carbon in oceanic and sedimentary carbon cycling. Geophys. Res. Lett. 19, 1851-1854. https://dx.doi.org/10.1029/92gl02159.

Canavan, R.W., Slomp, C.P., Jourabchi, P., Van Cappellen, P., Laverman, A.M., van den Berg, G.A., 2006. Organic matter mineralization in sediment of a coastal freshwater lake and response to salinization. Geochim. Cosmochim. Ac. 70, 2836-2855. https://dx.doi.org/10.1016/j.gca.2006.03.012.

Cole, T.M., Wells, S.A., 2006. CE-QUAL-W2: A Two-Dimensional, Laterally Averaged, Hydrodynamic and Water Quality Model, Version 3.5. User Manual. p. 680.

Dale, A.W., Sommer, S., Lomnitz, U., Bourbonnais, A., Wallmann, K., 2016. Biological nitrate transport in sediments on the Peruvian margin mitigates benthic sulfide emissions and drives pelagic N loss during stagnation events. Deep Sea Research Part I: Oceanographic Research Papers 112, 123-136. 10.1016/j.dsr.2016.02.013.

Dalsgaard, T., Thamdrup, B., 2002. Factors controlling anaerobic ammonium oxidation with nitrite in marine sediments. Appl Environ Microbiol 68, 3802-3808. https://dx.doi.org/10.1128/aem.68.8.3802-3808.2002.

Jørgensen, B.B., Revsbech, N.P., 1985. Diffusive boundary layers and the oxygen uptake of sediments and detritus1. Limnol. Oceanogr. 30, 111-122. https://dx.doi.org/10.4319/lo.1985.30.1.0111.

Schulz, H.D., 2006. Quantification of Early Diagenesis: Dissolved Constituents in Pore Water and Signals in the Solid Phase. In: Schulz, H.D., Zabel, M. (Eds.), Marine Geochemistry. Springer Berlin Heidelberg, Berlin, Heidelberg, pp. 73-124. https://dx.doi.org/10.1007/3-540-32144-6_3.

Wang, Y.F., VanCappellen, P., 1996. A multicomponent reactive transport model of early diagenesis: Application to redox cycling in coastal marine sediments. Geochim. Cosmochim. Ac. 60, 2993-3014. https://dx.doi.org/10.1016/0016-7037(96)00140-8.

Ward, B.B., 1986. Nitrification in Marine Environments. In: Prosser, J.I. (Ed.), Nitrification. IRL Press, Oxford, pp. 157-184.

**Fig. S1** Variations in the salinity and river discharge (Loire and Vilaine) (a, e), temperature and dissolved $O_2$ (b, f), $NO_3^-$ + $NO_2^-$ and $NH_4^+$ (c, g), Chl *a* in the water column and sediment surface (d, h), at the Ouest Loscolo monitoring station in 2015 (left) and 2016 (right) from January to December. Dashed-dotted horizontal line (panels a & e): hypoxia threshold (63 µM; Middelburg and Levin, 2009; Zhang et al., 2010). Vertical lines: dates of the sediment investigations.

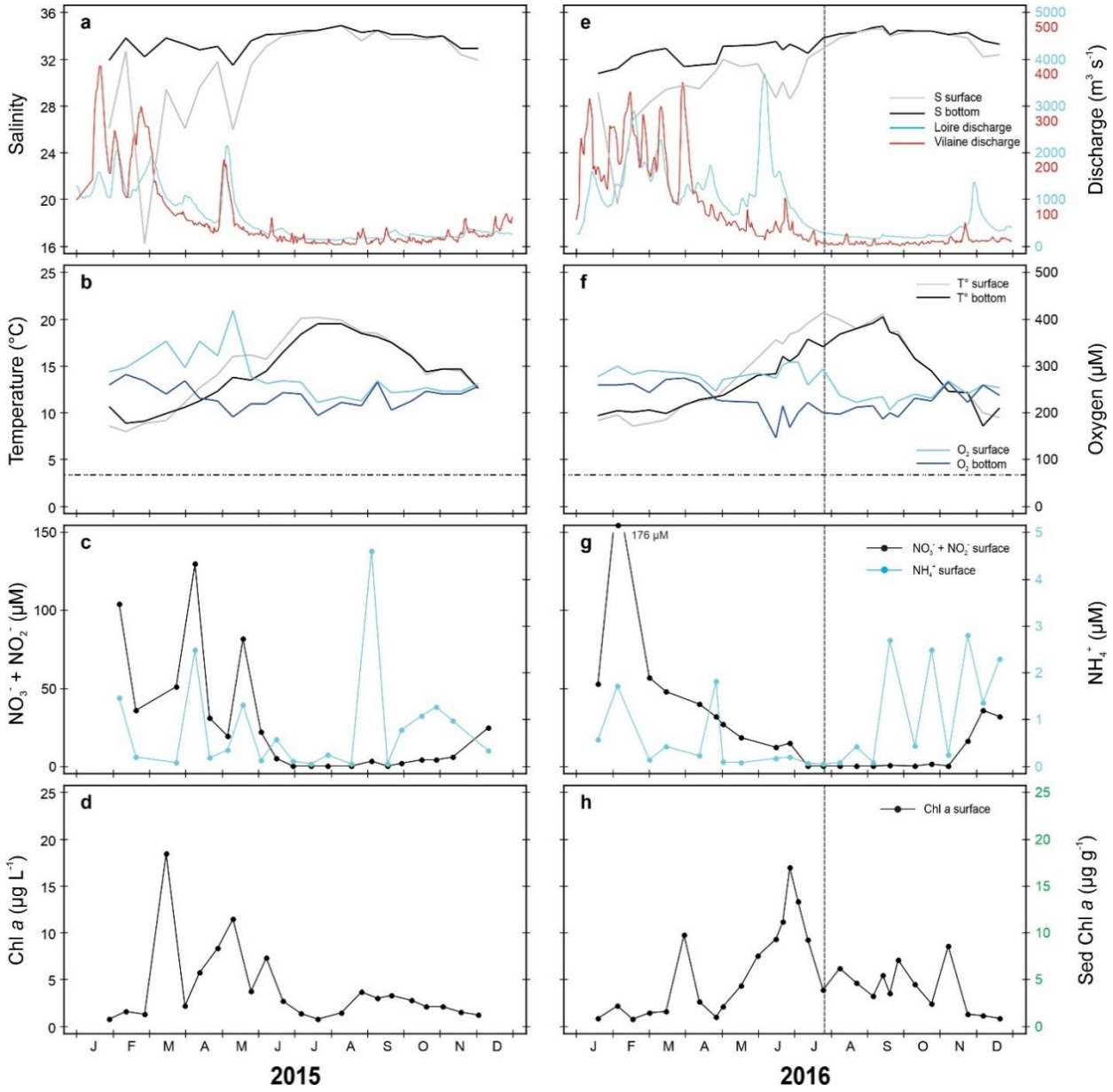

**Fig. S2** Depth profile of the grain size distribution at the Nord Dumet monitoring station (St. A) in triplicate sediment cores for the temporal study from April to September 2015. The y-axis represents each section of the sediment layers in the triplicate cores.

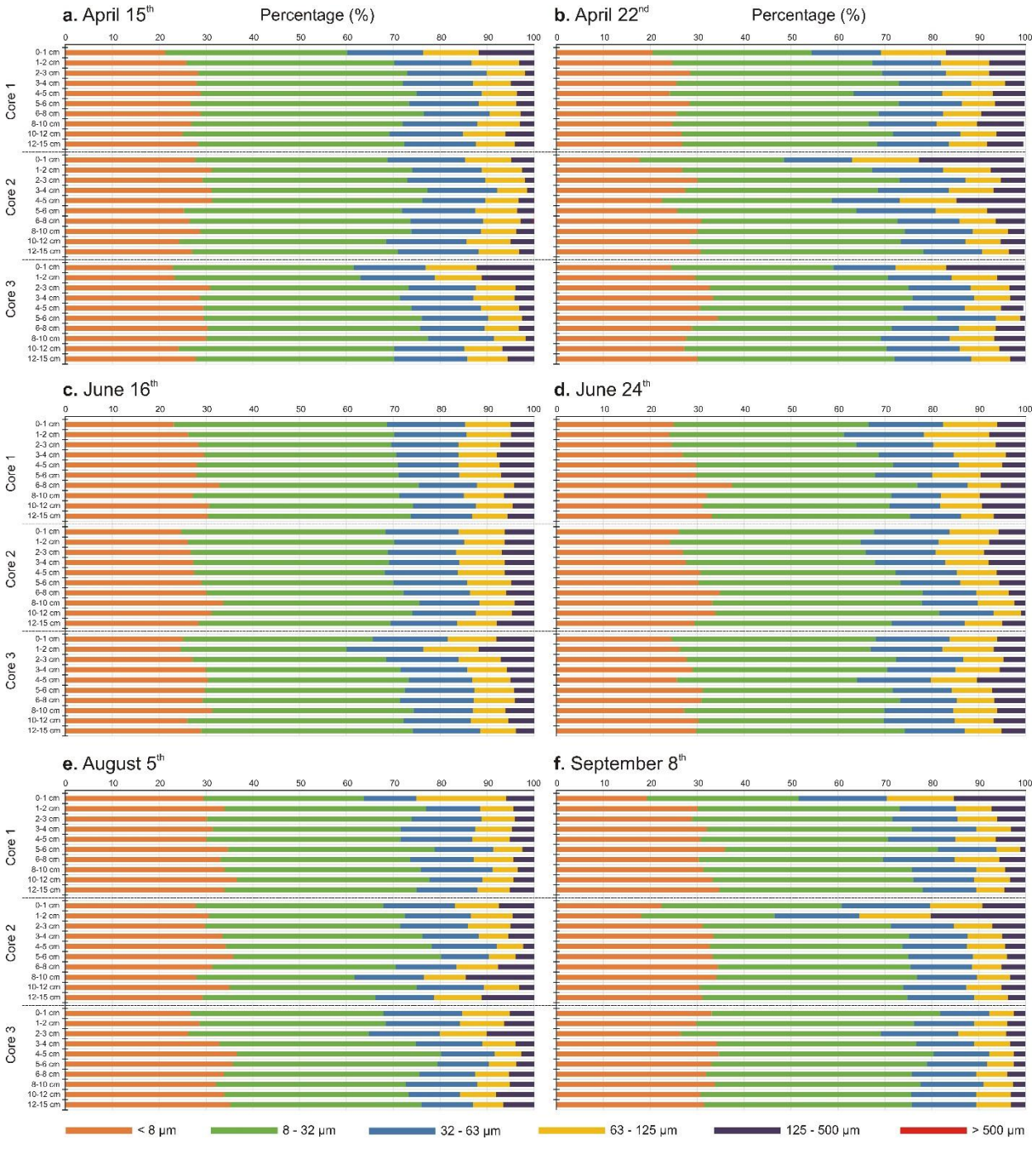

**Fig. S3** Depth profile of the grain size distribution in the triplicate sediment cores at Station A, B & C for the spatial study carried out in July 2016. The y-axis represents each section of the sediment layers in the triplicate cores. Right panel: image of a sediment core sampled at Station D. There was no analysis of the grain size distribution for Station D.

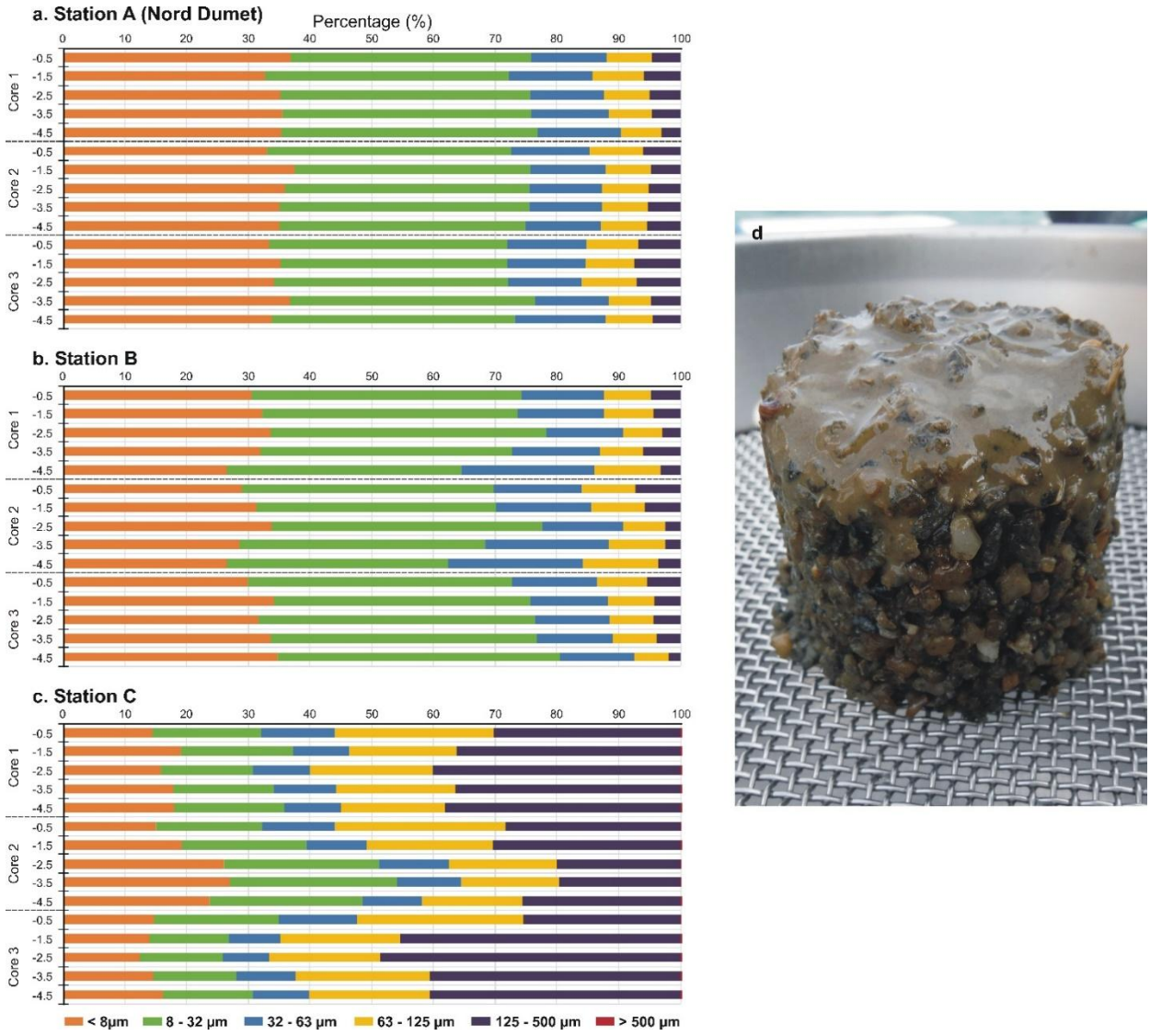

**Fig. S4** Depth profiles of the sediment porosity (a) and density (b) at the Nord Dumet monitoring station (St. A) for the temporal study carried out from April to September 2015. The solid horizontal lines are the standard error of the triplicate sediment cores. The red curves are the average of all of the values with the standard error (*n = 60*).

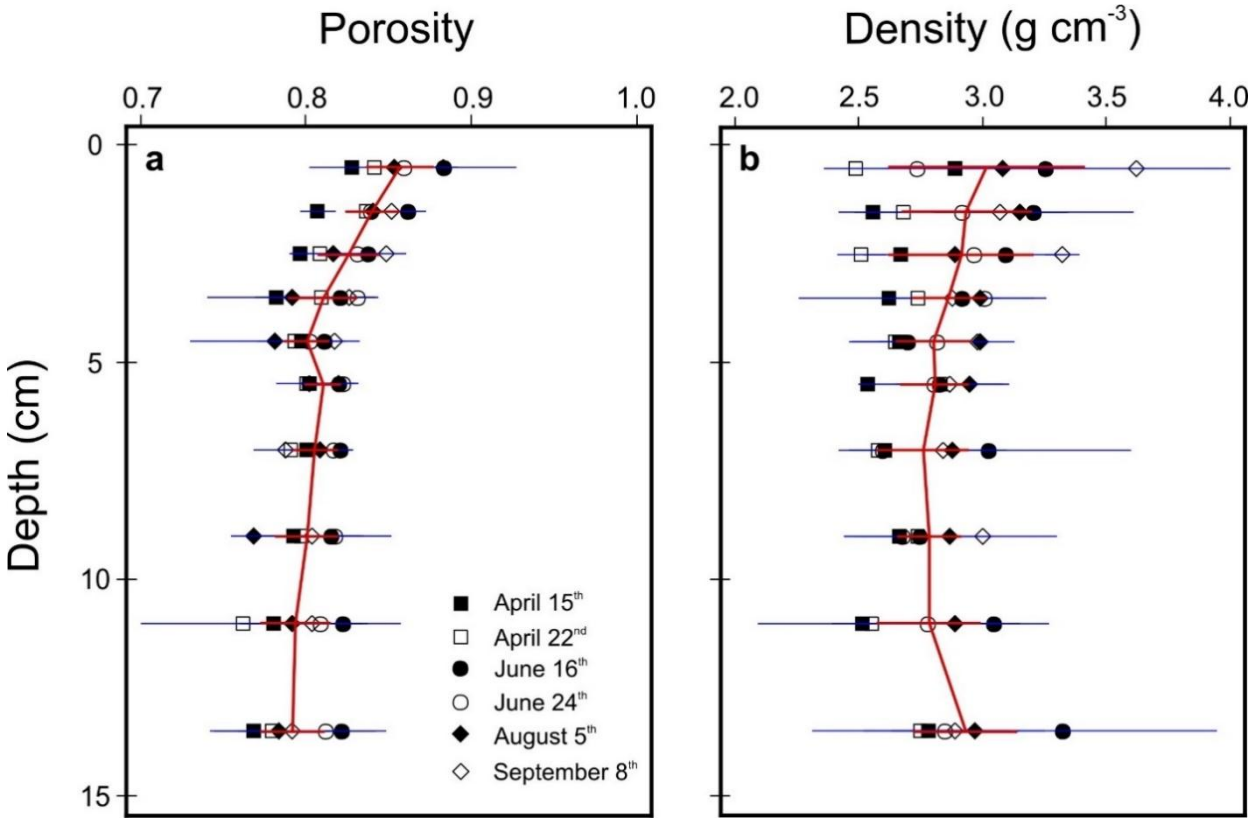

**Fig. S5** Depth profiles of the sediment porosity (a) and density (b) at Station A, B & C for the spatial study carried out in July 2016. The solid horizontal lines are the standard error of the triplicate sediment cores. Note: there was no measurement for Station D (gravel).

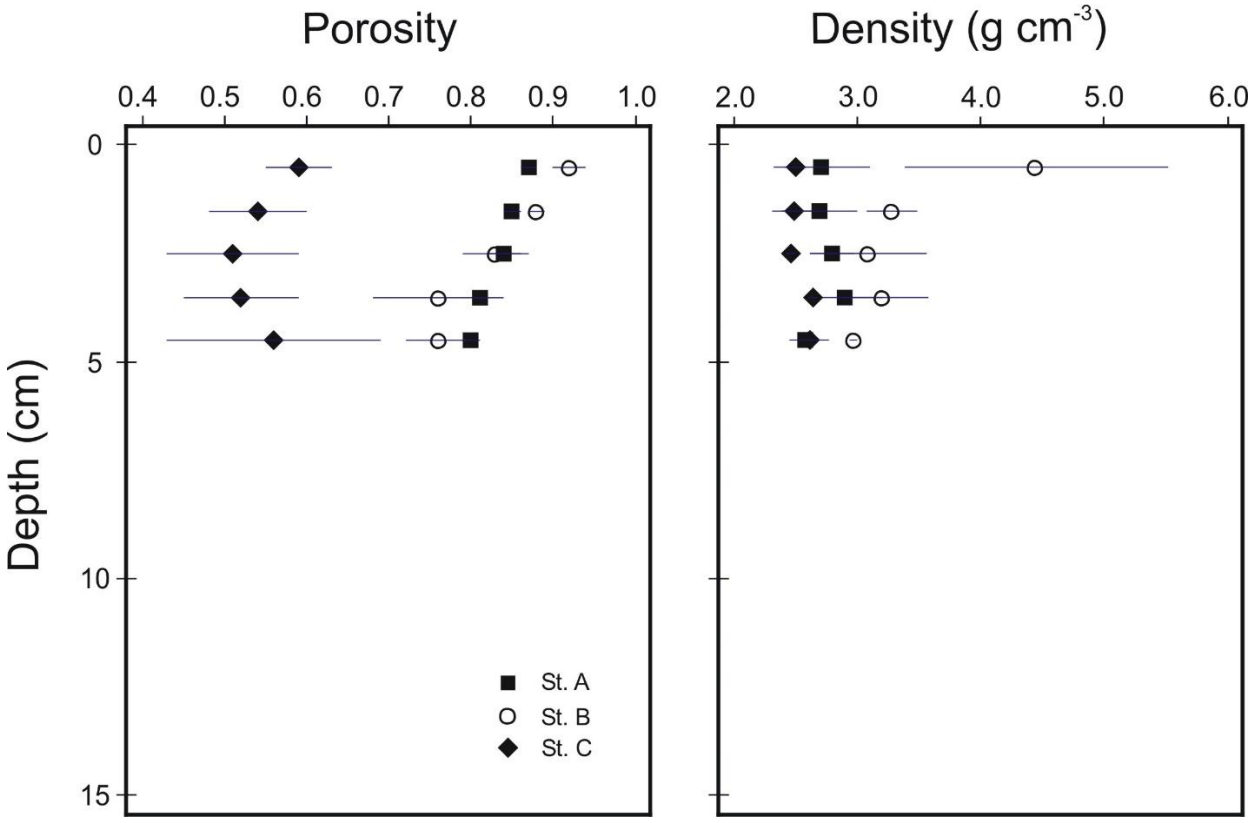

**Fig. S6** Concentrations of $C_{org}$, total N, BSi (in µmol $g^{-1}$) and Chl *a* (in µg $g^{-1}$) at the sediment surface (5 cm and 1 cm for Chl *a*) in April 2016. The data was interpolated using an automatic weighted-average gridding with the Ocean Data View software.

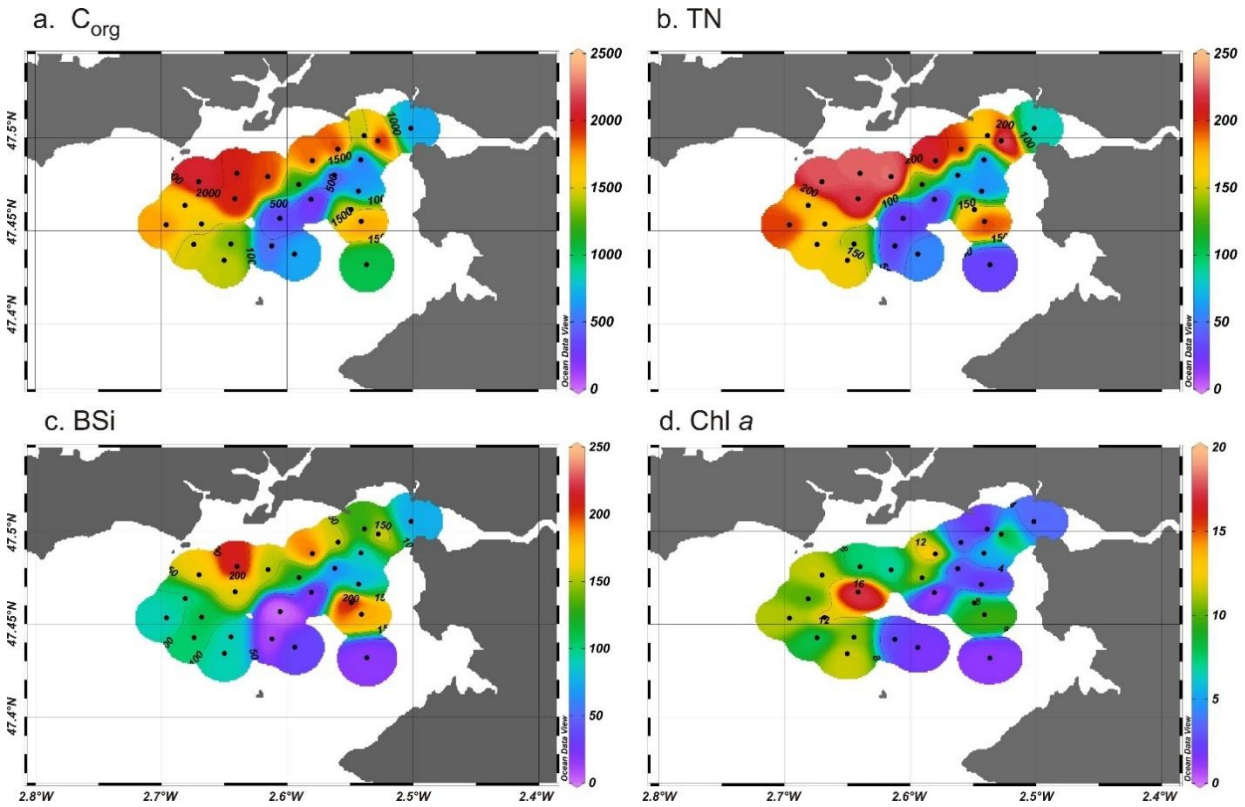

**Fig. S7** DON depth profiles at the Nord Dumet monitoring station (St. A) for the temporal study carried out from April to September 2015 (a) and global average of the measured DON and $NH_4^+$ values (b). The solid horizontal lines are the standard error of the triplicate sediment cores.

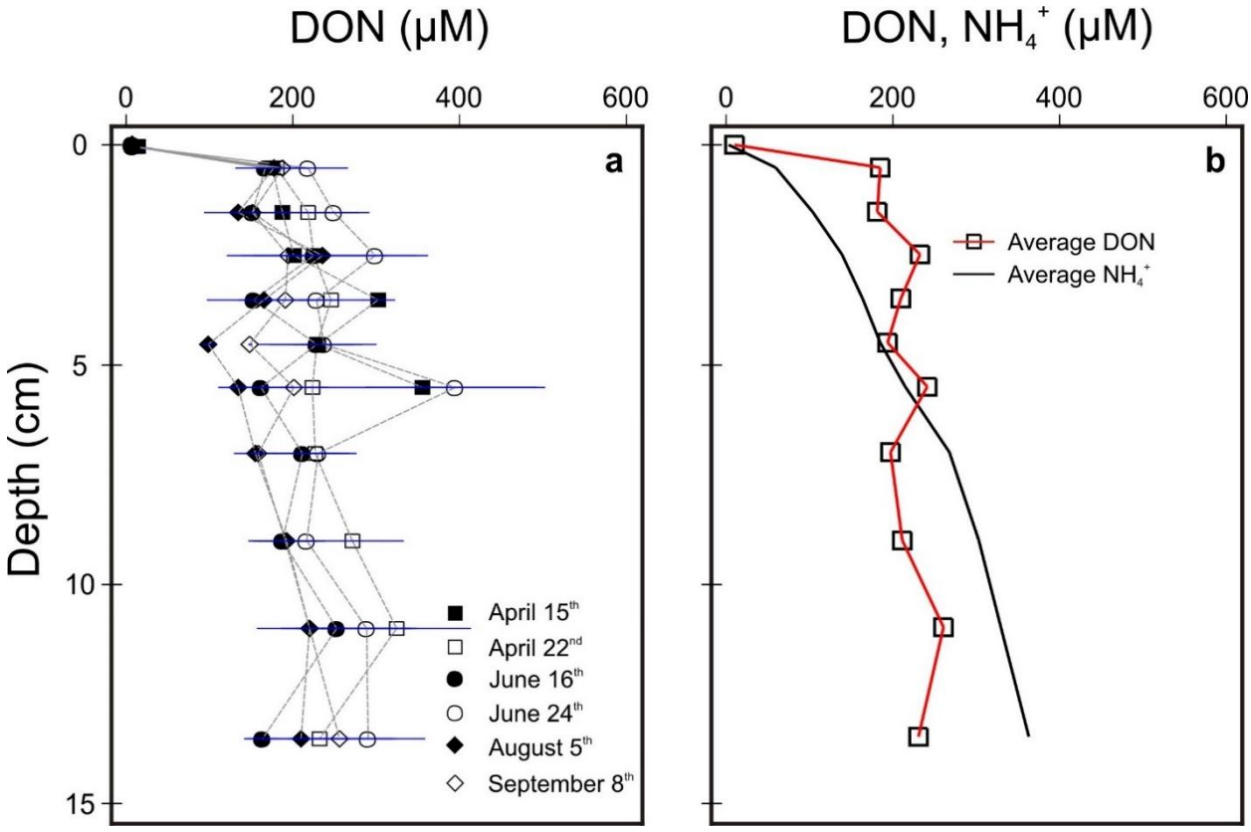

**Fig. S8** Microscopic observation of microalgae cells on the surface sediment at the Nord Dumet monitoring station (St. A) during the period of study from April to June (a) and from August to September (b) 2015.

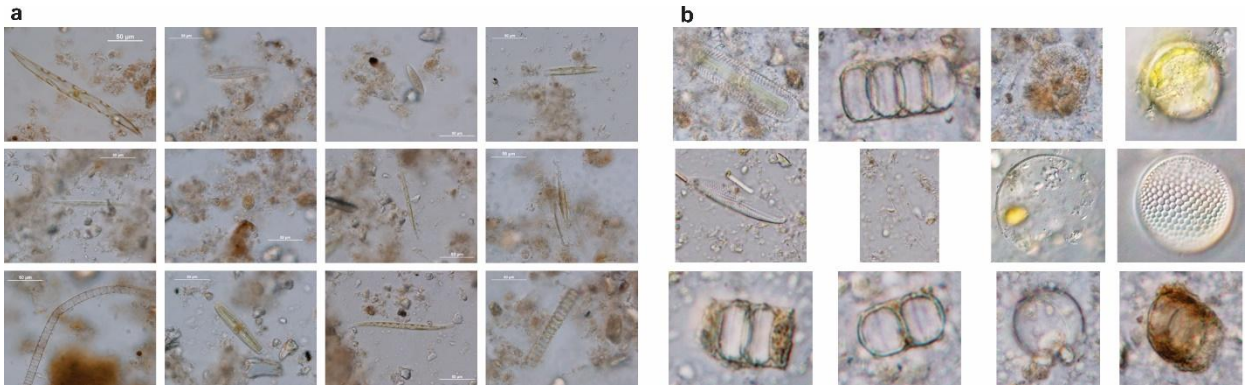

161

**Fig. S9** Modeled $NH_4^+$ fluxes in 2015 across the SWI as a function of the various *f*DNRA values. The various colored lines with the colored symbols represent the sampling dates. The solid symbols are the $NH_4^+$ fluxes measured at the Nord Dumet station.